final report

Project code: P.PIP.0431

Prepared by: G.E. Gardner[a], J. Peterse[a], S. Starling[b], J. Cook[b], M. Shirazi[b], A. Williams[a]
[a]School of Veterinary and Life Sciences, Murdoch University, Western Australia
[b]Scott Automation and Robotics Pty Ltd, Rydalmere, NSW

Date published: 5 June 2017

PUBLISHED BY
Meat and Livestock Australia Limited
Locked Bag 1961
NORTH SYDNEY NSW 2059

Beef DEXA Supply Chain Grading – LMY (Stage 2)

Final Report – Public Release

This is an MLA Donor Company funded project.

Meat & Livestock Australia acknowledges the matching funds provided by the Australian Government to support the research and development detailed in this publication.

Executive summary

A prototype DEXA system was purpose-built in a shipping container (DEXA-in-a-box; DIAB) to enable mobility and capacity to seamlessly modify the hardware without interrupting abattoir processing. The dimensions of this DEXA prototype were modelled on the JBS Bordertown DEXA system
This DEXA system demonstrated good potential for predicting CT composition, describing 93%, 88%, and 73% of the variation in whole carcase CT bone%, fat% and lean%, with RMSE values of 0.81 CT bone% units, 3.21 CT fat% units, and 3.49 CT lean% units. When predicting specifically within the forequarter and hindquarter regions, the precision was similar to whole carcase levels in the forequarter, but reduced in the hindquarter, describing about 10% less of the variation in composition.

The processing factors of spray-chilling or variation in carcase orientation had little impact on the DEXA prediction of composition. This suggests that this measurement will be robust within abattoir environments, and this coupled with its precision indicate that it is highly relevant for adoption by industry for the measurement of lean meat yield.

Table of contents

1 Background

The completion of work on a range of New Zealand lambs has proven conclusively that DEXA can provide objective lean, fat and bone characteristics that although not at CT accuracy (the gold standard) is the next best thing and verges on the entry point of objective carcase measurement with respect to Lean Meat Yield (LMY) and Saleable Meat Yield (SMY).

Scott Dual Energy HOT & COLD X-ray (DEXA) Full Beef Carcase System - Potential Evaluation (In New Zealand) – Stage 1.

Five (5) beef sides were purchased from Silver Fern Farms (as the beef sides would exit the food chain as pet food or landfill). They were scanned with an existing Scott-SFF Lamb DEXA system in New Zealand, both in their hot and cold state, then the same five sides sent to be scanned with a CT machine in New Zealand (the quarters having been cut into further small sizes to fit within the restrictions of the CT scanner). Graham Gardner of Murdoch University then analysed the three sets of data (i.e. hot DEXA, cold DEXA and CT) to ascertain the following:

1. There is better accuracy on hot over cold carcases
2. There is better accuracy on a whole carcase CT lean calculation than at the smaller part primal level.
3. All carcase CT lean from a lamb DEXA unit has a R^2 greater than 0.90. That is, based on the five sides of beef a greater than 90% whole of beef side CT lean equivalence can be measured. It was also observed that this percentage decreases significantly when measurements are extracted at a smaller primal level.

Further research, adoption and/or commercialisation strategy

Stage 2 of this project will define the additional DEXA hardware/software enhancements required to produce a purpose-built DEXA at a beef processing facility. A cost effective beef quarter DEXA scanner (mobile unit in a shipping container) will be built and located at a meat processing facility. This mobile unit will be used to undertake additional analysis on Australian cattle stock ranges via a mobile beef DEXA scanner and after the second data set of fifteen sides are scanned to validate the results from the first five sides scanned.

This Phase 2 study is likely to help define the additional DEXA hardware/software enhancements required to produce a purpose-built beef DEXA. Further work will also be required to develop algorithms for predicting SMY from DEXA outputs, stability of the DEXA measurements under a range of different environmental scenarios (ie. impact of carcase temperature, dehydration etc), programs for integrating the DEXA outputs into the supply chain, as well as the required training of supply chain participants.

Scott would then also be able to determine with more certainty:

- Does Beef DEXA have a chance of providing SMY information and other related information in either the hot and/or cold location?
- What is the $RRP of a beef DEXA system (including footprint)? How long would the first system take to be installed in a facility in Australia and provide reliable data that can be provided to livestock buyers for decision making?

2 Project Objectives

2.1 Project Sponsor Objectives

This project is sponsored by Meat and Livestock Australia [MLA] for the purpose of providing Teys Cargill Australia Pty Ltd (Teys) concise information with respect to deciding to invest in the predictive model approach to Lean Meat Yield (LMY) or to include (or upgrade in the future) a DEXA system along with the Scott SEXA Beef Cutting concept (in a hot and/or cold processing environment).

Scott is to provide a mobile, cost effective, fit for purpose (temporary) system to undertake additional analysis on Australian cattle stock ranges via a mobile Beef DEXA scanner.

Scott will also own and be free to operate the DEXA in a container system independent of the MLA project stakeholders at the completion of the MLA project stage 2.

2.2 Overall Project Objectives

The ultimate aim of Stage 1 and 2 still remains to address the questions of:

1. Is Beef DEXA a viable tool as an entry level into Objective Carcase Measurement specifically for LMY?
2. What is the accuracy of DEXA compared with predictive models?
3. How long will it take to get the first Beef DEXA system installed at Teys and at what cost?
4. What are the differences in placing a system in either the hot or cold carcase location?

2.3 Milestones as specified in Research Agreement

Milestone 1: System Design (with budget and timeframe revision)
Milestone 2: Order components
Milestone 3: Build and Scott workshop Demonstration
Milestone 4: Ship, Install and commission (and software support for Stage 1)
Milestone 5: Perform Phase 1 Trial – 8 Sides
Milestone 6: Perform Phase 2 Trial – 100 Sides
Milestone 7: Analyse DEXA and CT results for Phase 2 Trial
Milestone 8: Final Report

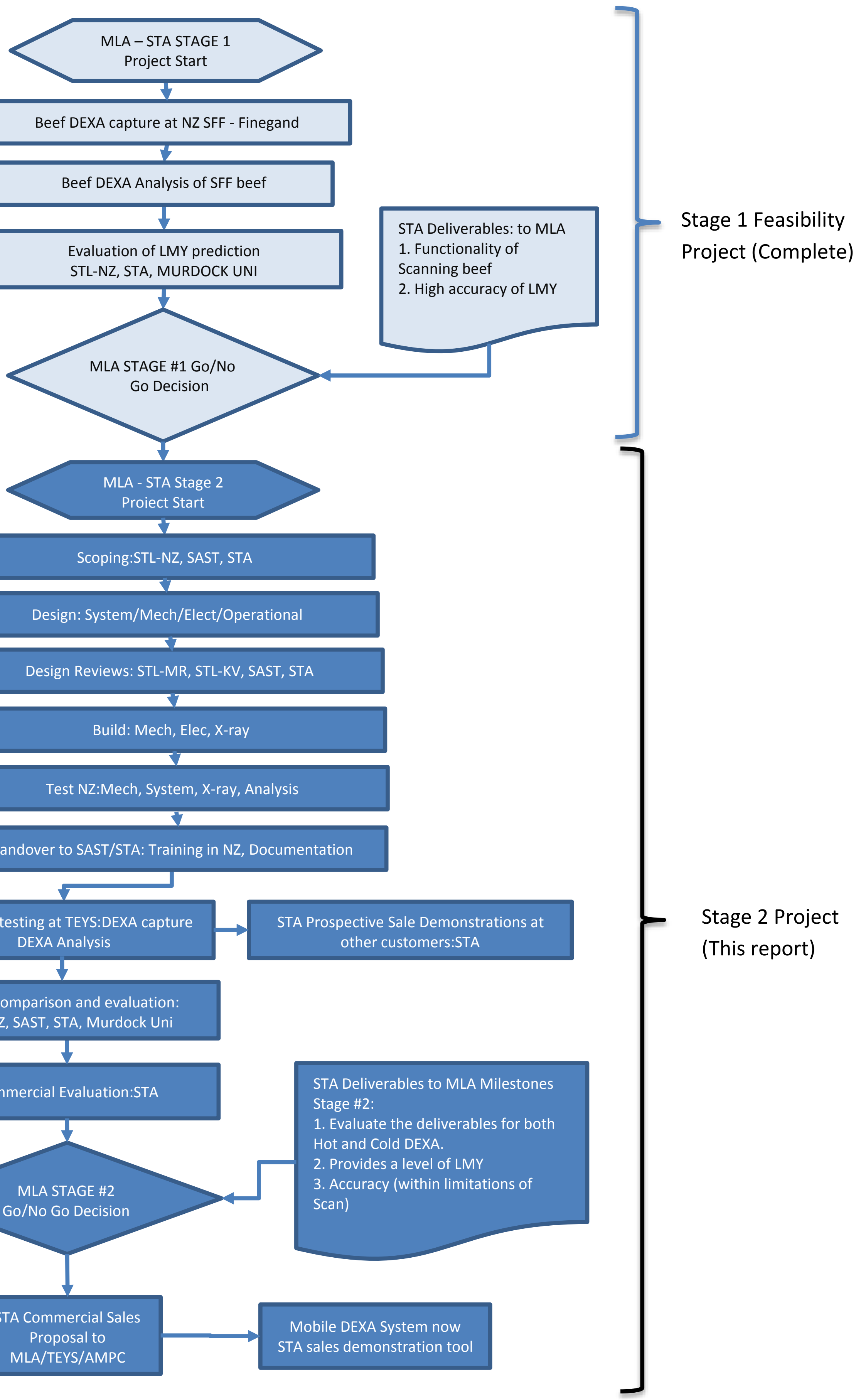

Figure 1: Project Methodology

3 Introduction

The current beef industry standard for determining carcase composition is based on carcase weight and a measurement of fat depth either on the hot carcase at the P8 site (located at the intersection of a line parallel to the spine from the tuber ischium and a line perpendicular to it from the spinous process of the third sacral vertebra (Johnston *et al.* 2003), or on the cold carcase at the rib quartering site between the 5^{th} and 13^{th} ribs (preferred by Meat Standards Australia; (Watson *et al.* 2008)). When predicting carcase yield both the 12^{th} rib and P8 measurements have been shown to be equally accurate when used in conjunction with hot carcase weight (Johnson 1987). However, the rib measurement is preferred by MSA due to other measurements being recorded at that site, such as eye muscle area, marbling and meat colour, and to ensure adequate fat cover over the expensive loin cuts (Watson *et al.* 2008). None-the-less, there is a perception within the Australian beef industry that these measures are inaccurate and lacking precision. Therefore alternative measurements of carcase composition are being explored.

One technology that can determine whole carcase composition with a high degree of accuracy is dual x-ray absorptiometry (DEXA) which makes use of R-values to reflect fatness. R-values are calculated when photons of two different energies are passed through an absorber, with attenuation of the lower energy expressed as a ratio (R-value) to attenuation observed at the higher energy (Peppler et al. 1981). These R-values align positively with atomic mass, thus in carcase images the bone-containing pixels which are higher in elements such as calcium and phosphorus will have R-values as much as 2-fold higher than soft-tissue pixels which themselves will vary on the basis of fat content (Pietrobelli et al. 1996). Therefore the bone-containing pixels can be eliminated from the carcase image, creating a 2-part mixture from which the percentage of muscle and fat can be calculated and body composition estimated.

The precision and accuracy of DEXA has been previously demonstrated in a number of meat animal species including lamb (Mercier et al. 2006; Pearce et al. 2009), pigs (Mitchell et al. 1998; Lukaski et al. 1999; Suster et al. 2003) and cattle (Mitchell et al. 1997) using off-the-shelf medical DEXA scanners. Yet to date this technology has not been applied for determining carcase composition within abattoirs, in part due to expense and the need for X-ray shielding, but also due to practical limitations associated with speed and carcass movement. Many of the modern medical devices acquire the high and low energy DEXA images by pulsing the X-ray tube (Pietrobelli et al. 1996). This mandates that the scanned object is held perfectly still to produce two matching high and low energy images, a problematic requirement in abattoirs where speed and carcase movement are the norm. To overcome this we utilised a “sandwich” style detector system that combines two photodiodes separated by a copper filter. A single emission from an X-ray tube passes through the first photodiode that is more responsive to low energy photons, then through the copper filter which attenuates the low energy photons, and finally through the second photodiode that is more responsive to high energy photons, enabling the acquisition of low and high energy images instantaneously. This system has been applied within lamb abattoirs and is also coupled with a robotic boning system (Scott Automation and Robotics Ltd.) that is capable of operating at 30 carcases per minute, 3-times the fastest chain speeds.

For beef, a prototype DEXA system has been purpose-built in a shipping container (DEXA-in-a-box; DIAB), matching the physical hardware and dimensions used within the lamb abattoirs. This test rig has been constructed to enable scanning of beef carcases, allowing optimisation of the design of a beef DEXA system. This study describes the precision for determining beef carcase composition using a prototype DEXA system in a group of 51 carcases.

4 Method

4.1 Animals, slaughter protocols and DEXA image acquisition

The prototype Teys DIAB hardware at the Brooklyn plant in Victoria was used to capture dual energy images of 51 beef carcases, scanned as four separate quarters.

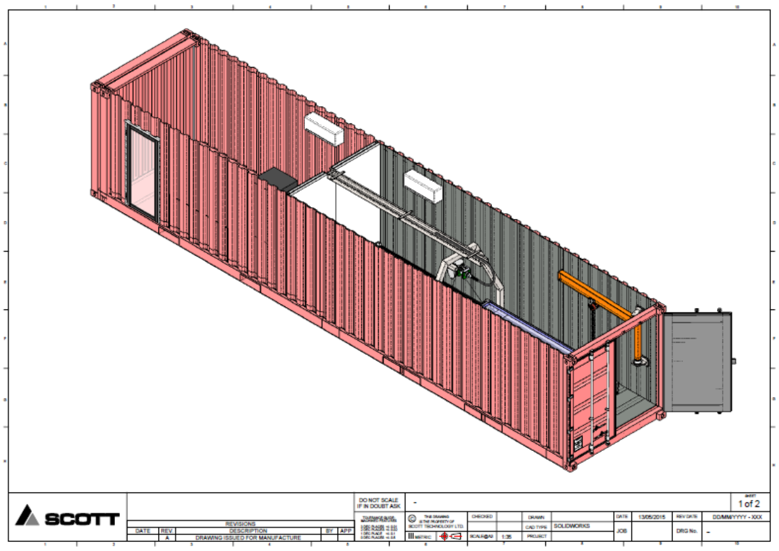

Figure 2: 40’ container – final design.

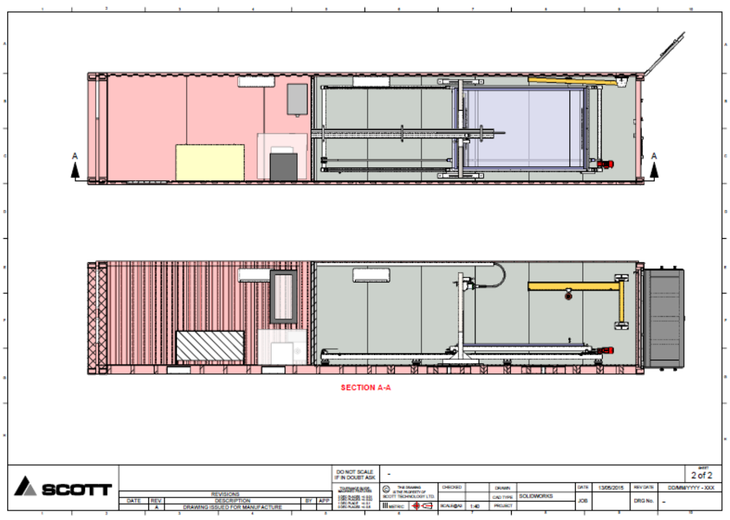

Figure 3: Container layout and foot print.

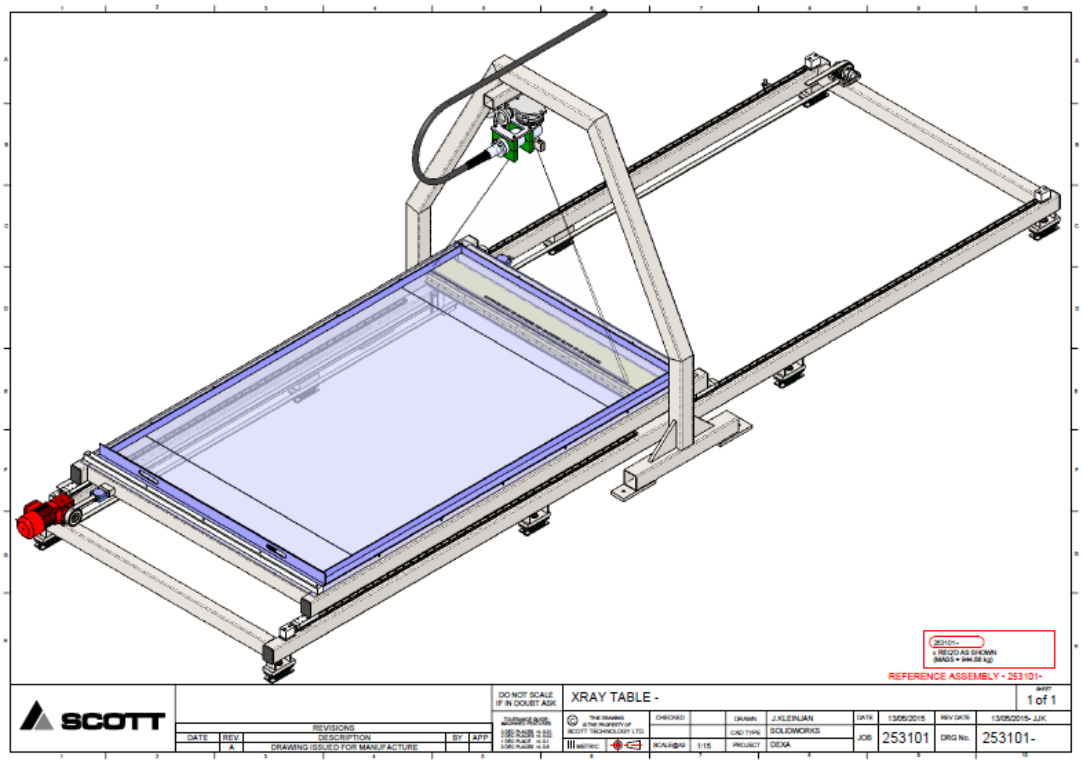

Figure 4: Moving table. This table will hold the beef and move from right to left while X-ray processed.

These carcases were from animals that had been slaughtered 1-2 days prior, and stored at 2˚C until scanning. During the chilling process half of each carcase, hung as a side, was spray-chilled and the other chilled conventionally. These carcase sides were then cut below the 12th rib and the quarters DEXA scanned in a flat position, oriented with the inside of the ribs facing upward (U). X-Ray images were generated using a single emission from a 140kV X-ray tube, with a set of two images captured using two photodiodes separated by a copper filter.

Figure 5 - Quarter being loaded for DEXA scanning.

The first photodiode used a scintillant that was more responsive to low energy photons, and the second used a scintillant that was more responsive to high energy photons. This system enabled the acquisition of high and low energy images of each carcase quarter which were then used to calculate an R-value for each pixel within these images according to the following formula:

$(R = \ln(I_{Low}/Air_{Atten}) / \ln(I_{High}/Air_{Atten}));$

Where: I_{Low} represents the pixel value in the low energy image
I_{High} represents the pixel value in the high energy image
Air_{Atten} represents the pixel value corresponding to the un-attenuated photons (I_0) in the white part of each image.

The average R-value for all of the pixels in the carcase quarter image was calculated, and the image was then reconstructed after removing any pixels with R-values lying above this mean R-value. Pixel R-values were then converted to proportion of lean tissue and weighted based on thickness using the equations derived in a previous report (see first MLA DIAB report), and then averaged to reflect an average R-value for each carcase quarter (see "DEXA Value" in Table 1). These carcase R-values were then used to predict CT lean%, fat%, and bone% which were measured directly on these same carcase quarters.

Within every DEXA image, a synthetic phantom consisting of nylon and perspex (calibration block) was also scanned. In this case a linear correction was applied to the average DEXA value of each image set based on the corresponding calibration block average R-value. However, upon analysis it was found that this correction did not improve the prediction of carcase composition. Therefore all reported DEXA estimates of composition have not been corrected for their value relative to the calibration block that was scanned within every image.

Additional DEXA scans were collected for the first 24 carcases slaughtered using the non-spray-chilled side only. The fore and hind quarters were scanned after re-orienting them to achieve a tilted angle of approximately 45˚, although still with the inside of the ribs facing upward (T), and then scanned again with the inside of the ribs facing down (D). Exactly the same image processing and analysis procedures were then undertaken as described above.

4.2 Computed tomography scanning

CT scanning of carcases was undertaken using a Seimens Sensation 64 spiral CT scanner to determine the proportions of fat, lean and bone. Prior to scanning the carcasses were split into 16 discrete primal regions that are aligned to commercially relevent cutting lines as shown in Figure 7.

Figure 6 - The beef carcases were broken down into 16 primals for CT scanning.

In part this was to meet the size limitations of the CT apperture but also will enable future analysis of CT composition data within these regions. For CT scanning the spiral abdomen protocol was selected with settings: pilot scan length of 512 mm, field of view set at 480mm, exposure 150mAs, Voltage 100kV,Current 180 mA, pitch 0.6. The carcasses were scanned in 5 mm slice widths, with each slice taken 5 mm apart.

The analysis of images produced from the CT scan was the same as that used by Anderson et al. (2015). In summary these images were edited to remove non-carcass image artefacts and were partitioned into bone, muscle and fat components (Image J version 1.37v, National Institutes of Health, Bethesda, MD, USA, used in conjunction with Microsoft Excel). The discrimination point to identify the Hounsfield barriers for associating pixels with fat, muscle and bone were –235 to 2.3 for fat, 2.4 to 164.3 for lean and >164.3 for bone. An estimate of volume using Cavalieri's method (Gundersen et al. 1987; Gundersen et al. 1988) was calculated as follows:

m

$$\text{Volume}_{Cav} = d \times \sum_{g=1} \text{area}_g - t \times \text{area}_{max}$$

in which m is the number of CT scans taken and d is the distance between cross-sectional CT scans, in this case 10 mm. The value of t is the thickness of each slice (g), in this example 10 mm, and area max is the maximum area of any of the m scans.

The average of the Hounsfield units of the pixels of each component was then determined and converted into density (kg/L) using a linear transformation (Mull 1984). This was then used along with the volume of each component to determine the weight of fat, lean and bone, which was then expressed as a percentage of total carcass weight at the time of scanning. Given the density of the marrow tissue, it is classified as either fat or lean using the boundary discrimination method described above. Additional editing within Image J enabled the isolation of the marrow component of bone within all images. Thus the above procedures could be repeated on the ‘marrow only’ images. This enabled back correction for these pixels, reallocating them as bone and removing their associated volumes from the lean and fat components of the first iteration of image analysis. Thus using the CT scans it is possible to determine the percentage of fat, lean and bone within each carcass.

4.3 Statistical Analysis

In order to explore the interaction of spray chilling, and the calibration block, on DEXA’s ability to predict CT composition linear mixed effects models were constructed with CT lean%, fat% or bone% within each quarter as the dependent variable. Fixed effects included spray chill (Yes/No) and carcase section (forequarter/hindquarter), and covariates included DEXA Value and calibration block R-value, with animal ID used as a random term to account for the multiple sampling of the same carcase. Covariates were also tested as curvilinear terms but were not significant.

General linear models were then constructed using the DEXA Value to predict CT lean%, fat% and bone% within the spray-chilled and non spray-chilled fore and hindquarters. This was then repeated wih the inclusion of weight of that quarter at scanning in the model. Again covariates were tested as curvelinear terms but were not significant.

In order to model a potential industry application, and because spray chilling was shown to have minimal impact on carcase composition, the CT lean%, fat% and bone% data from both the spray-chilled and non spray-chilled fore and hind quarters were reconstructed into one whole carcase. These measurements of whole carcase CT lean%, fat% and bone% were then predicted using separate DEXA values from the four carcase quarters and hot carcase weight as covariates in a general linear model.

Lastly, linear mixed effects models were constructed to determine the impact of carcase scanning orientation on the ability of DEXA to estimate carcase composition. In this case CT lean%, fat% and bone% were dependent variables, carcase orientation (U,D,T) was included as a fixed effect, and DEXA Value as the covariate.

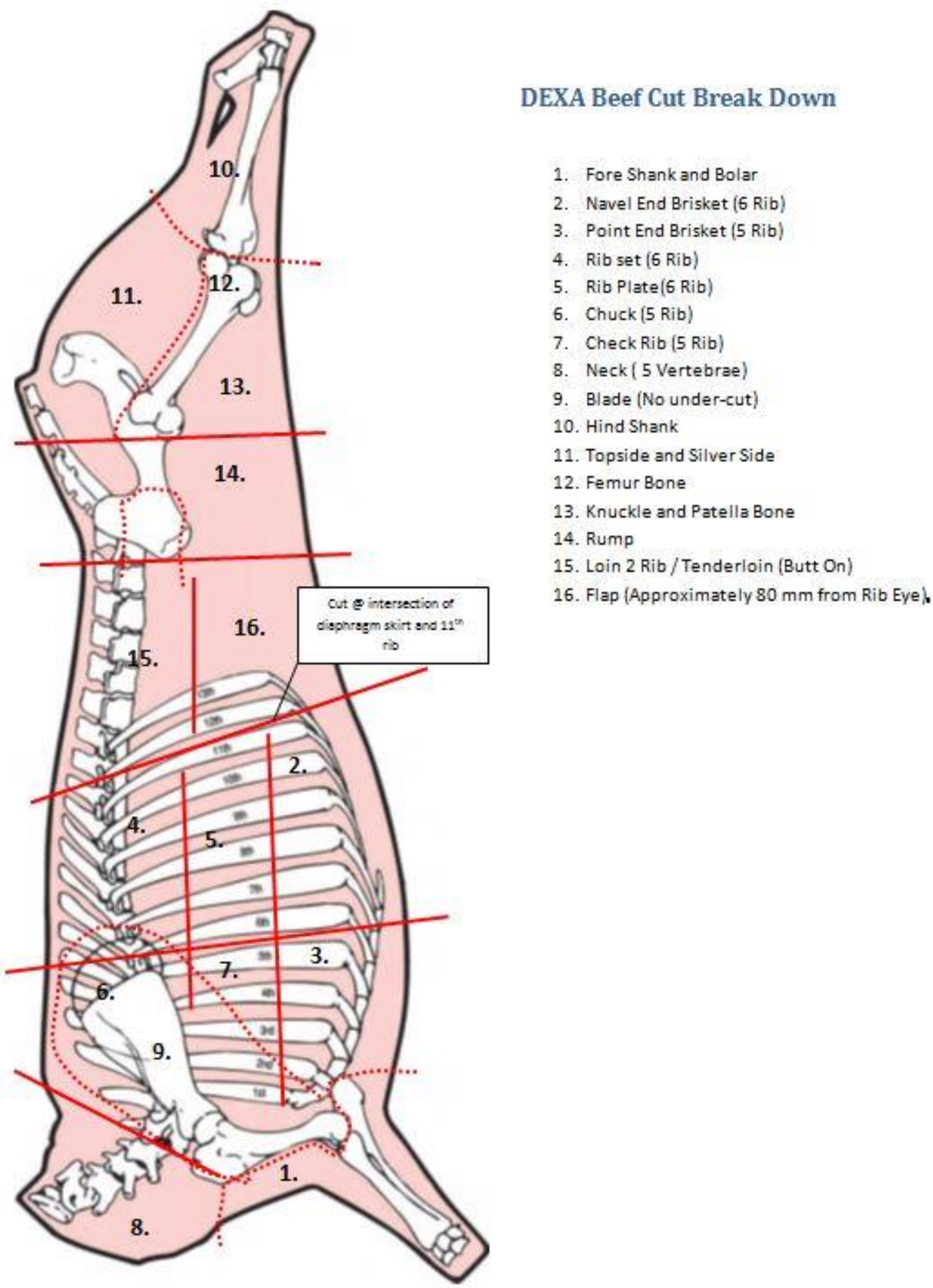

Figure 7 - Cutting regions for CT scanning

5 Results

Descriptive statistics of the carcases scanned are shown in Table 1 below. The intention was to scan carcases across a diverse range of weight and fatness (selected based upon P8 fat depths).

Table 1 - Descriptive statistics for key traits. Values are mean ± standard deviation (min, max).

		No Spray-Chill					Spray-Chill			
		Mean	StDev	Min	Max		Mean	StDev	Min	Max
CTLean %	Forequarter (n=51)	58.76	6.34	41.19	74.73	Forequarter (n=51)	58.44	6.35	38.86	72.75
CTFat %		22.88	8.65	7.61	45.54		23.01	8.77	8.69	48.39
CTBone %		18.36	3.13	13.27	26.49		18.55	3.30	12.75	28.13
DEXAValue		64.07	23.65	7.66	118.59		61.51	23.55	1.17	116.57
quarter Wt (kg)		79.52	17.96	40.76	114.74		80.88	18.40	44.01	122.36
CTLean %	Hindquarter (n=51)	65.27	6.62	40.91	77.62	Hindquarter (n=49)	64.95	6.74	40.01	77.14
CTFat %		19.01	8.64	6.22	48.46		19.44	8.65	6.64	49.30
CTBone %		15.71	2.72	10.62	22.60		15.61	2.63	10.69	22.78
DEXAValue		26.96	23.07	-37.32	80.55		27.91	21.19	-18.54	82.03
quarter Wt (kg)		71.59	16.58	35.91	117.23		72.11	16.13	38.09	111.95
CTLean %	Full side (n=51)	61.84	6.40	41.05	76.04	Full side (n=49)	61.50	6.54	39.41	74.77
CTFat %		21.06	8.59	6.98	47.02		21.31	8.75	7.75	48.82
CTBone %		17.10	2.90	11.93	24.67		17.19	2.97	11.77	24.82
DEXAValue		42.87	23.37	-22.79	96.65		41.72	22.23	-15.41	94.56
side Wt (kg)		153.98	34.94	78.00	233.50		153.91	35.27	81.00	238.50
HSCW (kg)	Carcase (n=51)	308.03	69.52	159.00	472.00	Carcase (n=49)	307.68	70.85	159.00	472.00
P8 fat		14.69	12.15	1.00	50.00		14.73	12.40	1.00	50.00

Correlations of DEXA values between carcase sections were high, with the forequarter sections correlating at 0.99 and the hind quarter sections showing a correlation of 0.93. Correlations between DEXA values and carcase weight at the time of CT scanning were lower and negative, ranging between -0.74 and -0.76.

Table 2 - Simple correlation coefficients between DEXA values of the left and right forequarter and left and right hindquarter sections of the carcase and cold carcase weight.

	Left Forequarter DEXA Value	Right Forequarter DEXA Value	Left Hindquarter DEXA Value	Right Hindquarter DEXA Value	Cold carcase weight at CT (kg)
Left Forequarter DEXA Value	1	0.99	0.95	0.95	-0.74
Right Forequarter DEXA Value	-	1	0.94	0.94	-0.76
Left Hindquarter DEXA Value	-	-	1	0.93	-0.76
Right Hindquarter DEXA Value	-	-	-	1	-0.74

Note: all correlations are significantly different from zero (P<0.05).

5.1 Effect of spray chill and association with synthetic phantom calibration block

Spray-chilling had a small impact on the DEXA estimated carcase composition, increasing CT lean% (P<0.05) on the fore and hindquarter sections by 0.3%, and decreasing CT bone% in the forequarter section only by 0.4% (Table 3). There were weak associations between the calibration block value and DEXA estimated carcase composition (Table 3), but only for CT lean% in the forequarter (P<0.1), and CT fat% in the forequarter (P<0.1). The calibration block R-values varied by as much as 0.024 units and across this increasing range CT lean% reduced by 2.0 units (Figure 8), and CT fat% increased by 2.9 units (Figure 9). A linear correction was applied to the average DEXA value of each image set based on the corresponding synthetic phantom value, however this did not improve the precision for any of the composition prediction equations reported below. Therefore this correction was not applied to the data in this study.

Table 3 - Models predicting CT Lean%, Fat% and Bone% in carcase quarters using forequarter and hindquarter DEXA values, with effects for spray chilling and nylon calibration block adjustment where significant. F-values, numerator and denominator degrees of free.

			CT Lean %		CT Fat%		CT Bone%	
			Coefficient ± SE	F-Value (NDF,DDF)	Coefficient ± SE	F-Value (NDF,DDF)	Coefficient ± SE	F-Value (NDF,DDF)
Intercept			72.4 ± 57.68	-	2.55 ± 60.424	-	13.3 ± 0.27	-
DEXAValue			0.046 ± 0.0158	8.26*** (1,146)	-0.104 ± 0.0168	38.7*** (1,147)	0.080 ± 0.0065	211.63*** (1,146)
Carcase Section	Fore		78.7 ± 45.80	2.95* (1,146)	-111 ± 47.8	5.43** (1,147)	-0.809 ± 0.2734	18*** (1,146)
	Hind		-	-	-	-	-	-
Spray-chill		No	0.294 ± 0.1631	3.26* (1,146)	-	-	0.222 ± 0.1159	1.86 (1,146)
		Yes	-	-	-	-	-	-
Cal. Block			-7.58 ± 50.253	0.81 (1,146)	17.0 ± 52.64	1.69 (1,147)	-	-
Cal. Block * Carcase Section	Fore		-75.6 ± 39.86	3.6* (1,146)	103 ± 41.6	6.19* (1,147)	-	-
	Hind		-	-	-	-	-	-
DEXAValue * Carcase Section	Fore		-	-	-	-	0.018 ± 0.0036	24.71*** (1,146)
	Hind		-	-	-	-	-	-
Carcase Section * Spray-chill	Fore	No	-	-	-	-	-0.665 ± 0.164	16.49*** (1,146)
	Fore	Yes	-	-	-	-	-	-
	Hind	No	-	-	-	-	-	-
	Hind	Yes	-	-	-	-	-	-

*, P<0.1; **,P<0.05; ***,P<0.01. In all cases animal ID as the random term was significant (P<0.01)

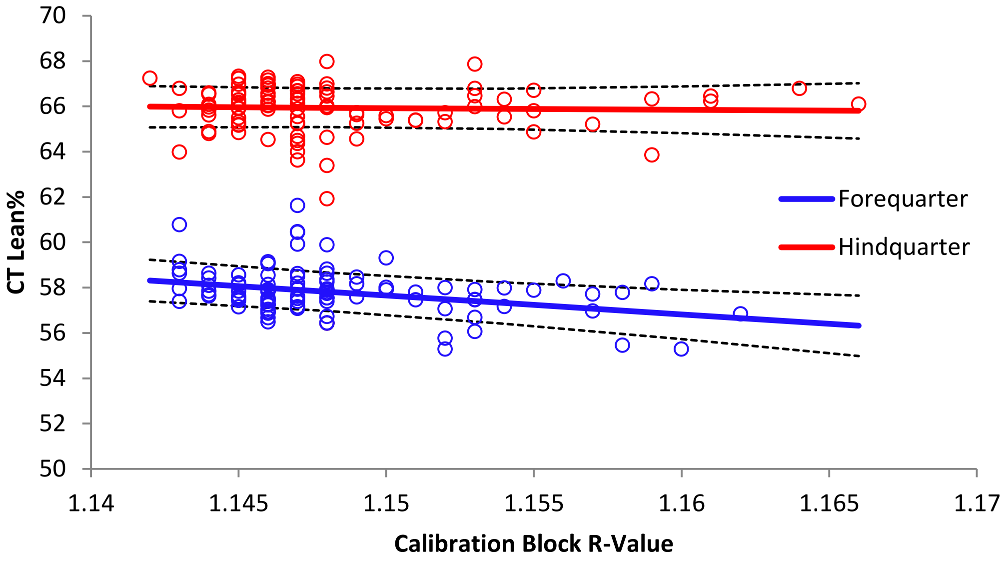

Figure 8 - Association between CT lean% and calibration block R-value in the forequarter and hindquarter sections of the carcase. Icons represent raw data, and lines are predicted means (±SE).

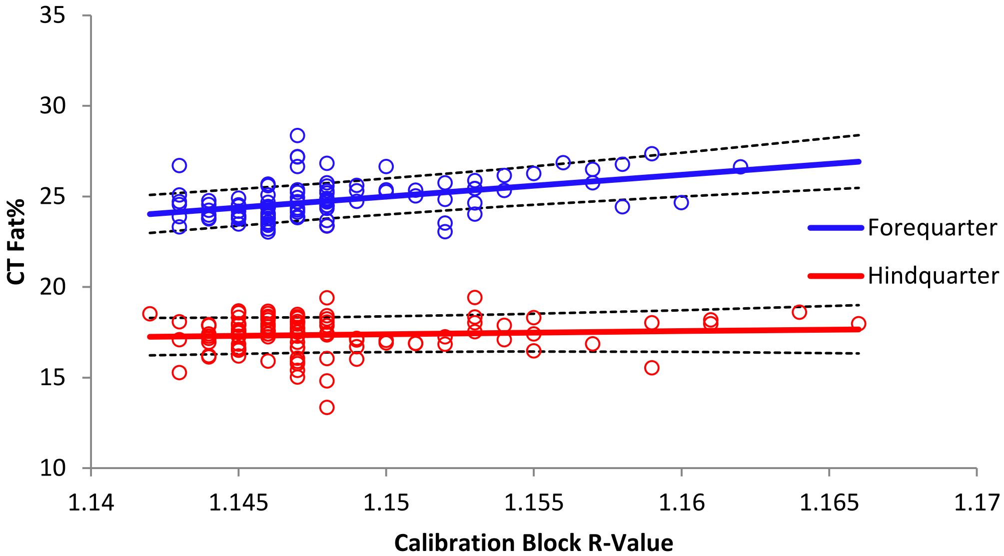

Figure 9 - Association between CT fat% and calibration block R-value in the forequarter and hindquarter sections of the carcase. Icons represent raw data, and lines are predicted means (±SE).

5.2 Predicting carcase composition

The prediction of CT composition varied between tissue types, and carcase sections, but relatively little when component weight was included in the model. The best results were those achieved for CT bone% and fat% within the full side and forequarter (see Table 4). In these cases the RMSE values were as low as 1.11 (R^2 = 0.87) for CT bone% (see Figure 10) and 3.48 (R^2 = 0.85) for CT fat% (see Figure 10) in the forequarter. This compares with standard deviations as high as 3.30 and 8.77 for CT bone% and fat%, indicating that DEXA has more than halved the error. Within the hind quarter precision was lower for CT bone% and fat% with RMSE values of 1.23 (R^2 = 0.79) and 4.21 (R^2 = 0.76) for these tissues (see Figure 10). This compares with standard deviations as high as 2.72 and 8.65 for CT bone% and fat%. When full sides were reconstructed the precision estimates were similar to the forequarter figures.

The precision estimates for the DEXA prediction of CT lean% followed a similar pattern between carcase sections as those for CT bone% and fat% although values were somewhat lower (see Table 4). Thus the RMSE values were only as low as 3.88 (R^2 = 0.63) in the forequarter, 4.10 (R^2 = 0.62) in the hind quarter, and 4.04 (R^2 = 0.63) for the reconstructed carcase side (see Figure 10). This compares with the standard deviations for CT lean% of 6.35, 6.74, and 6.54 in the forequarter, hindquarter and full carcase side.

In most cases when component weight was included in the prediction model the precision changed very little (see Table 4). The only exception to this was for CT bone%, with R^2 values showing small increases in the forequarter, hindquarter, and full side, the largest increase being 0.05 units to an R^2 value of 0.93 (RMSE = 0.83) in the full side model (see Figure 10).

In most cases there was relatively little difference in the precision of DEXA prediction of carcase composition between spray-chilled and non-spray-chilled sides (see Table 4). The main outliers to this were for the hindquarter CT lean% and fat% prediction with better precision shown in the spray-chilled sides by 12-14%, and by 11% for these two tissues (see Figure 10).

Table 4 - Models predicting CT Lean, Fat and Bone % in forequarter and hindquarter carcase sections, and then in reconstructed (composite) full side images for both the spray chilled and non-spray chilled sides. Models are shown for predicting composition using just the DEXA value, and using both DEXA value and the weight of the component (ie forequarter, hindquarter or whole side weight). F-value, intercept and coefficients are reported for each model, as well as estimates of precision (R2, root-mean-square-error (RMSE)).

			Non Spray Chill				Spray Chill			
			no wt component		wt included		no wt component		wt included	
			Coef	F Value	Coef	F Value	Coef	F Value	Coef	F Value
CT Lean %	Forequarter	Intercept	45.7		43.7		45.5		43.9	
		DEXAValue	0.205	68.4**	0.214	33.3**	0.211	77.1**	0.219	38.1**
		Wt component	-	-	0.017	0.11	-	-	0.014	0.09
		R-Square	0.58		0.58		0.61		0.61	
		Root MSE	4.138		4.176		4.001		4.039	
	Hindquarter	Intercept	59.2		65.3		58.9		68.9	
		DEXAValue	0.226	80.6**	0.2	19.4**	0.2	41.9**	0.153	9.34**
		Wt component	-	-	-0.071	1.460	-	-	-0.114	2.96
		R-Square	0.62184		0.632973		0.471761		0.50374	
		Root MSE	4.11		4.09		4.95		4.85	
	Full side	Intercept	54.2		54.9		46.8		49.5	
		DEXAValueFQ	0.044	0.360	0.044	0.340	0.268	13.6**	0.259	11.9**
		DEXAValueHQ	0.2	5.42*	0.17	4.66*	-0.1	0.6	-0.07	0.72
		Wt component	-	-	-0.004	0.020	-	-	-0.013	0.260
		R-Square	0.63		0.63		0.62		0.62	
		Root MSE	3.97		4.01		4.12		4.15	
CTFat %	Forequarter	Intercept	43.9		49.8		44.0		51.6	
		DEXAValue	-0.329	205.5**	-0.357	110.8**	-0.341	257.8**	-0.379	154.2**
		Wt component	-	-	-0.051	1.3	-	-	-0.066	2.84
		R-Square	0.81		0.81		0.84		0.85	

		Root MSE	3.836		3.825		3.539		3.474	
	Hindquarter	Intercept	27.8		26.5		28.6		22.7	
		DEXAValue	-0.3	157.6**	-0.3	51.9**	-0.3	86.6**	-0.3	29.2**
		Wt component	-	-	0.015	0.060	-	-	0.067	0.900
		R-Square	0.763		0.763		0.648		0.655	
		Root MSE	4.25		4.29		5.19		5.19	
	Full side	Intercept	36.8		40.5		43.2		46.6	
		DEXAValueFQ	-0.2	6.39*	-0.19	6.61*	-0.4	33.00**	-0.40	32.72**
		DEXAValueHQ	-0.152	4.20*	-0.169	4.71*	0.065	0.750	0.057	0.550
		Wt component	-	-	-0.019	0.560	-	-	-0.017	0.480
		R-Square	0.81		0.81		0.82		0.82	
		Root MSE	3.867		3.885		3.793		3.814	
CTBone%	Forequarter	Intercept	10.4		6.4		10.5		4.5	
		DEXAValue	0.124	362.2**	0.143	252.3**	0.1302036	306.9**	0.160	297.2**
		Wt component	-	-	0.034	8.36**	-	-	0.052	19.2**
		R-Square	0.881		0.899		0.862		0.902	
		Root MSE	1.09		1.02		1.24		1.06	
	Hindquarter	Intercept	13.0		8.15		12.5		8.42	
		DEXAValue	0.1	135.7**	0.1	96.78**	0.1	174.6**	0.1	137.2**
		Wt component	-	-	0.056	8.72**	-	-	0.047	9.22**
		R-Square	0.73		0.78		0.79		0.82	
		Root MSE	1.413356		1.31371		1.225689		1.13081	
	Full side	Intercept	8.94		4.58		10.0		3.87	
		DEXAValueFQ	0.138	51.92**	0.144	71.69**	0.117	37.14**	0.136	80.5**
		DEXAValueHQ	-0.025	1.62	-0.004	0.05	-0.001	0.00	0.014	0.7
		Wt component	-	-	0.023	14.57**	-	-	0.030	32.1**
		R-Square	0.88		0.91		0.87		0.93	
		Root MSE	1.025		0.905		1.084		0.837	

** P< 0.05; *, P< 0.1.

	CT Lean %	CT Fat %	CT Bone %
Non Spray Chill Forequarter	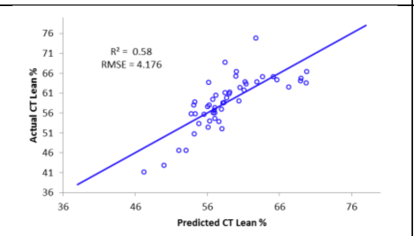	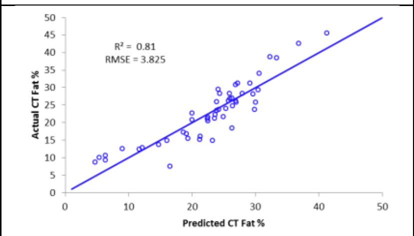	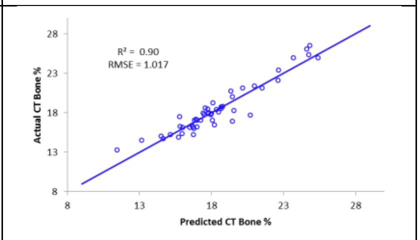

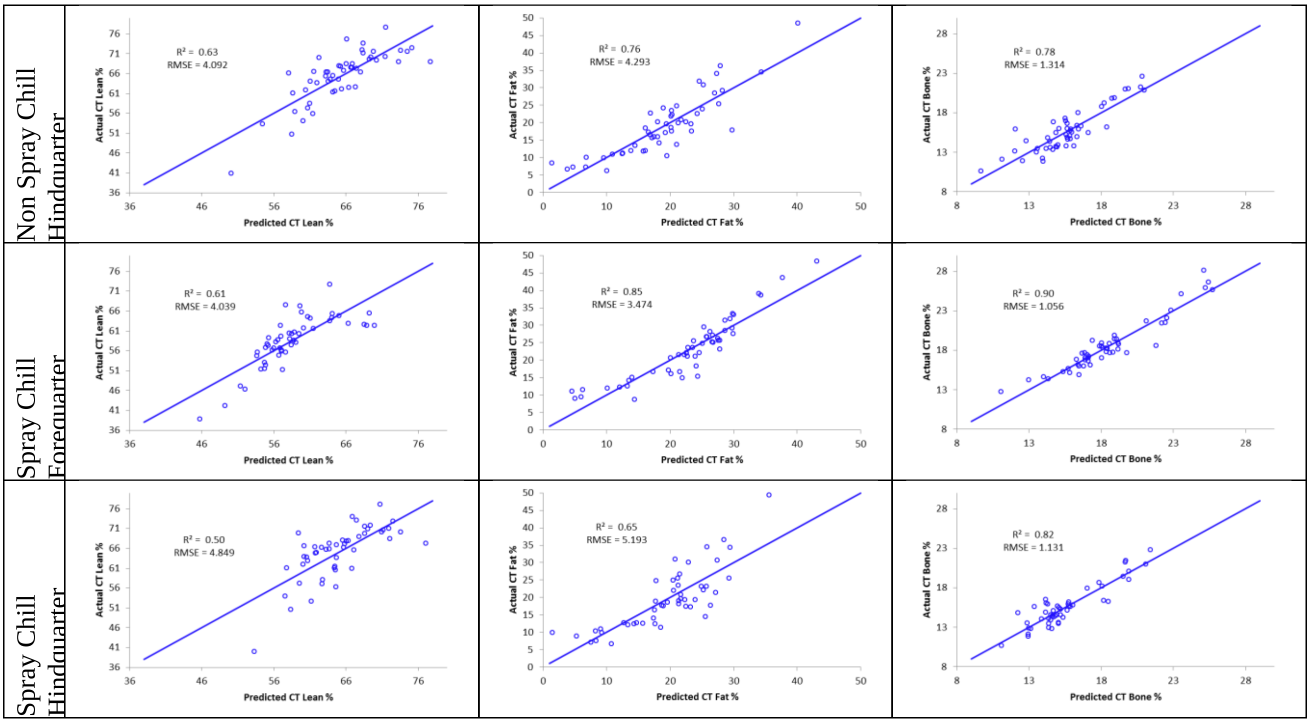

Figure 10 - Association between CT lean%, fat%, and bone% (in columns) with spray-chilled and non-spray-chilled forequarter and hindquarter sections of carcases and the corresponding DEXA prediction of these values. Icons represent raw data, and lines are depicte d on a 45degree angle where the data would all fit if the prediction was perfect.

Given the limited effect of spray chilling, CT data from carcase sections were reconstructed into full carcases to determine whole carcase CT composition. This was then predicted using DEXA values from each carcase quarter and carcase weight. In this case there was little change in precision for the prediction of CT Fat% (Table 5; Figure 12; Figure 11) and Bone% (Table 5; Figure 13), although a marked improvement in CT Lean% (Table 5; Figure 11) with R^2 value of 0.73 (RMSE = 3.48).

Table 5 - Models predicting CT Lean, Fat and Bone % in reconstructed full carcases using forequarter and hindquarter DEXA images from both carcase sides and carcase weight as predictors. F-value, intercept and coefficients are reported for each model, as well as estimates of precision (R^2, root-mean-square-error (RMSE)).

	CTLean %		CTFat %		CTBone%	
Intercept	55.0		44.6		3.98	
DEXAValue (left forequarter)	-0.573	14.63**	0.510	13.1**	0.086	7.37**
DEXAValue (Right forequarter)	0.624	21.2**	-0.712	30.4**	0.059	3.31*
DEXAValue (left hindquarter)	0.171	6.33*	-0.186	8.05**	-	-
Carcase wt at CT (kg)	-	-	-0.023	4.49*	0.013	26.8**
R-Square	0.73		0.88		0.93	
RMSE	3.486		3.212		0.810	

** P< 0.05; *, P< 0.1.

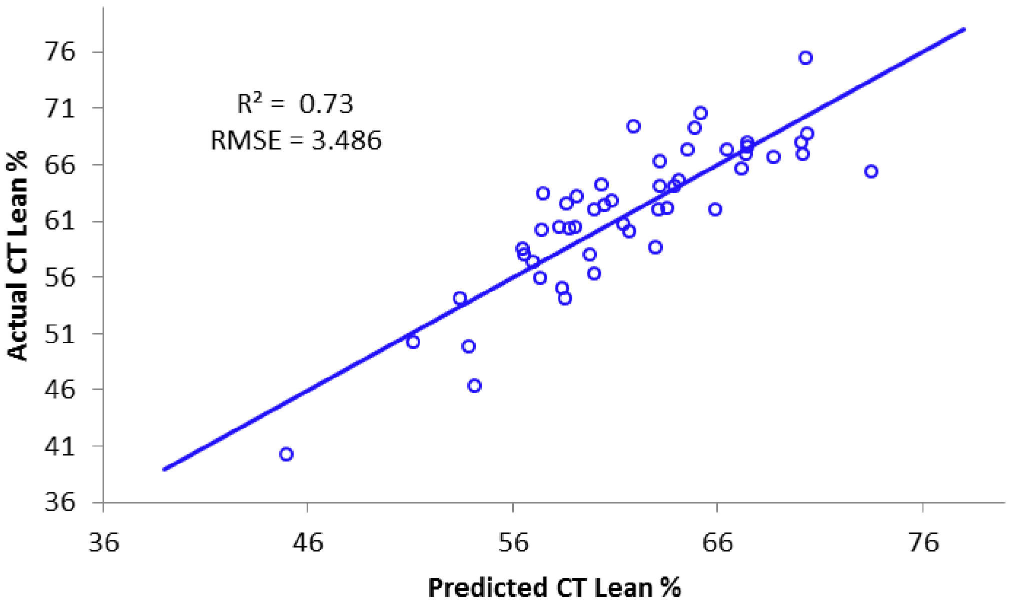

Figure 11 - Association between CT lean% in a whole carcase and DEXA-predicted CT lean% with the prediction derived from the forequarter and left hindquarter sections and hot carcase weight. Icons represent raw data, and lines are predicted means (±SE).

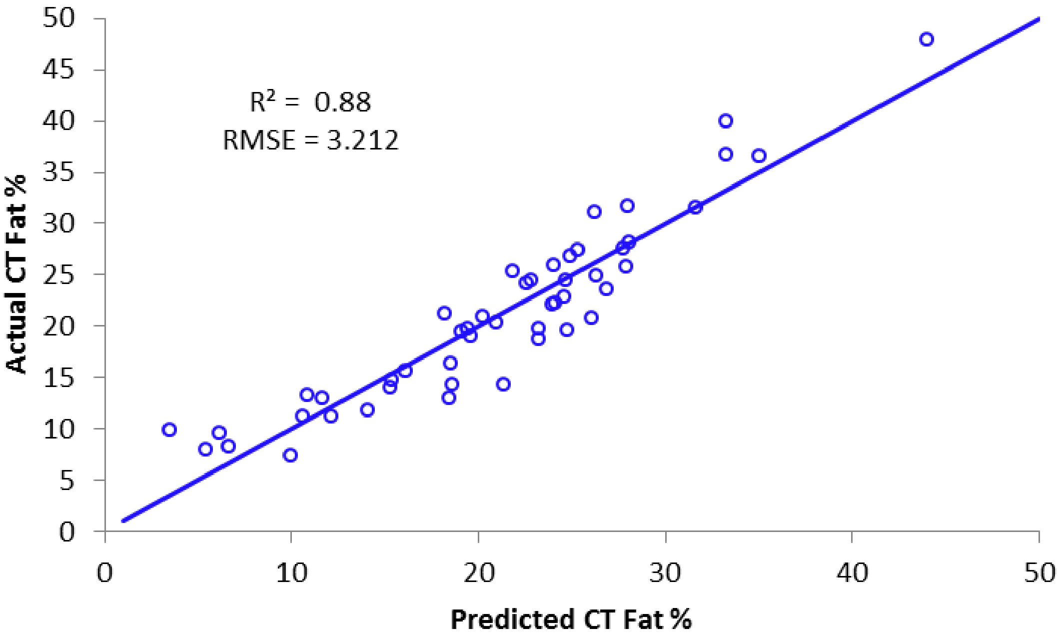

Figure 12 - Association between CT fat% in a whole carcase and DEXA-predicted CT fat% with the prediction derived from the forequarter and left hindquarter sections and hot carcase weight. Icons represent raw data, and lines are predicted means (±SE).

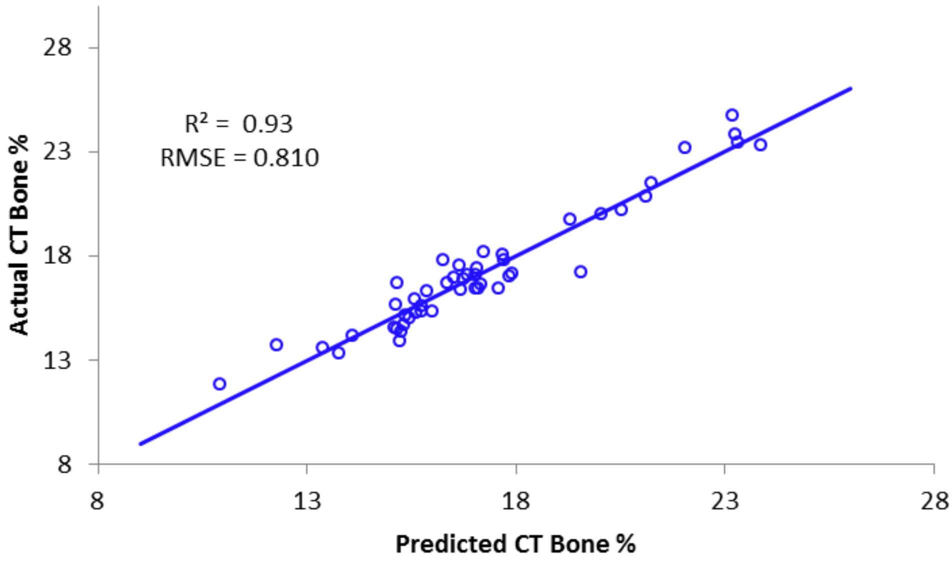

Figure 13 - Association between CT bone% in a whole carcase and DEXA-predicted CT bone% with the prediction derived from the forequarter and left hindquarter sections and hot carcase weight. Icons represent raw data, and lines are predicted means (±SE).

5.3 Effect of scanning orientation on DEXA values

The non-spray-chilled side from the first 24 carcases sourced were scanned multiple times across a range of orientations. Descriptive statistics of this sub-set of carcases are shown in Table 6 below. Although not as extensive as the full data set, there was still a diverse range of weight and fatness (selected based upon P8 fat depths) within this group.

Table 6 - Descriptive statistics for key traits of carcases that were scanned across multiple orientations. Values are mean ± standard deviation (min, max).

		Mean	Std Dev	Minimum	Maximum
CTLean %	Forequarter (n=24)	60.27	3.67	54.00	66.38
CTFat %		20.17	7.07	8.72	30.78
CTBone %		19.56	3.74	14.87	26.49
DEXAValue (up)		71.10	26.97	38.50	118.59
DEXAValue (down)		64.31	28.42	18.88	115.09
DEXAValue (tilted)		71.93	33.54	31.33	130.87
quarter Wt (kg)		83.20	18.72	40.76	114.02
CTLean %	Hindquarter (n=24)	66.88	3.51	61.10	72.50
CTFat %		15.90	6.13	6.67	25.42
CTBone %		17.22	2.89	13.35	22.60
DEXAValue (up)		34.03	24.50	-6.29	80.55

DEXAValue (down)	41.90	26.22	-1.01	87.09
quarter Wt (kg)	73.61	15.94	35.91	100.19

There were small differences between orientations (Table 7). The current manufacturing orientation is brisket facing up (U). A 180 degree change in orientation relative to this position, such that the brisket was facing down (D), produced small shifts in estimated bone composition of 0.82% in the forequarter and -0.80% in the hindquarter. These orientation effects were not significant for the other tissue types, and in all cases there were no effects of tilting the carcase component by 45degrees while in the brisket facing up position (T).

Table 7 - Models predicting CT Lean%, Fat% and Bone% in carcase quarters using forequarter and hindquarter DEXA images aquired across a range of different orientations including up, down, and tilted. F-value, intercept and coefficients are reported for each model, as well as estimates of precision (R^2, root-mean-square-error (RMSE)).

		Forequarter		Hindquarter	
		Coefficient	F Value	Coefficient	F Value
CTLean %	Intercept	53.3		63.2	
	DEXA Value	0.097	113.7**	0.109	74.1**
	Orientation D	0.662	0.770	-0.859	1.810
	Orientation T	-0.081		0	
	Orientation U	0		-	
	R-Square	0.63		0.62	
	Root MSE	2.262		2.184	
CTFat %	Intercept	35.7		23.1	
	DEXA Value	-0.218	357.6**	-0.211	143.3**
	Orientation D	-1.479	2.420	1.657	3.500
	Orientation T	0.180		0	
	Orientation U	0		-	
	R-Square	0.84		0.76	
	Root MSE	2.849		3.029	
CTBone %	Intercept	-		13.8	
	DEXA Value	0.120	735.1**	0.101	174.3**
	Orientation D	0.817	4.97**	-0.798	4.26*
	Orientation T	-0.099		0	
	Orientation U	0		-	
	R-Square	0.92		0.79	
	Root MSE	1.097		1.323	

Simple correlations were also estimated for the DEXA values within section between each orientation. Within the forequarter the correlation between the “up” and “down” orientations was 0.99. The correlations between the “up” and “down” orientation and the “tilted” orientation was 0.98 and 0.97. In the hindquarter, where only the “up” and “down” orientations were tested, the correlation was 0.97.

6 Discussion

6.1 Precision of predicting CT bone%, muscle%, and fat%

The beef DEXA system demonstrated good precision for predicting the composition of bone and fat, describing as much as 93% and 88% of the variation in whole carcase CT bone% and fat%. While these are acceptable results, it should be noted that the data range (which heavily influences R^2) was large, extending across 41.8 CT fat% units and 13 CT bone% units. The root mean square error (RMSE) for these traits was 3.21 CT fat% units and 0.81 CT bone% units, with 4 times these values (which is equivalent to the range across which 95% of the actual data lies from the predicted value) representing 31% and 25% of the raw data range. This precision needs to be put in context of the yearly distribution of animals slaughtered within commercial abattoirs. Few data of this type exist, hence future work will need to include benchmarking of predicted CT fat% composition of cattle populations slaughtered within Australian abattoirs. None-the-less we can put this range of CT fat% into context with commercial figures by crudely reflecting its association with P8 fat depth within the animals used in this study, as shown in Figure 14 below. Thus a 42 unit range in CT fat% was associated with a 49 mm range in P8 fat depth, which for come plants is quite comparable to the magnitude of variation seen within an individual days kill.

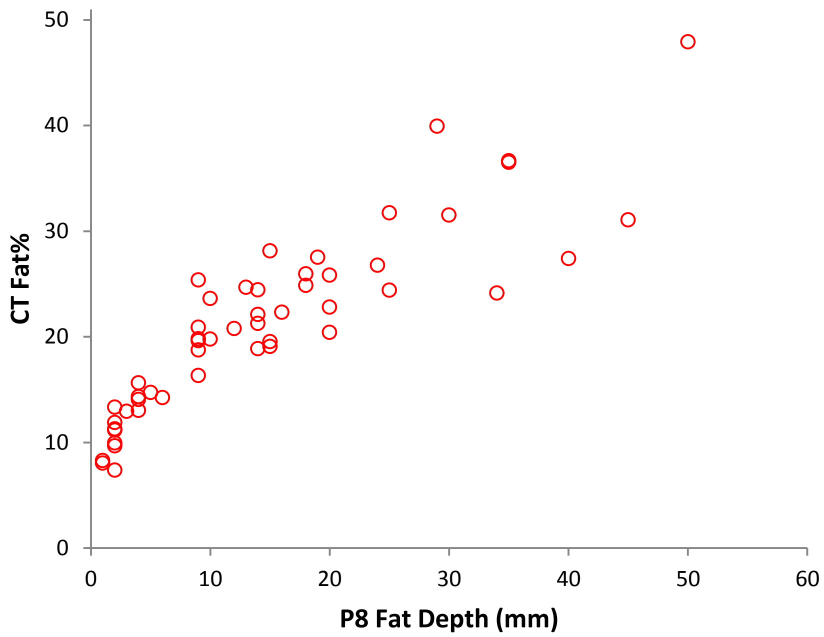

Figure 14 - Raw data representation of CT fat% and P8 fat depth.

In contrast to CT fat% and bone%, the precision of prediction of CT lean% was somewhat less, describing only 73% of the variation with an RMSE of 3.49 CT lean% units. Four times this RMSE value (distribution of 95% of data around prediction) represented 38% of the 36.6 unit range in CT lean%.

The predictive power of the beef DEXA system compares reasonably well to the lamb DEXA system, describing a similar amount of variation in composition within the training data set. However its precision (reflected through the RMSE values) was less, with values that were double that of lamb. In the lamb study previously reported (see MLA project report No A.MQA. 0017) the RMSE values for predicting CT fat%, lean%, and bone% were 1.42, 1.69, and 0.80. The corresponding fat%, lean% and bone% ranges (min to max) were 23.7, 19.5, and 9.86, thus four times the RMSE represented 24%, 35%, and 32% of the range of CT fat, lean and bone. It should be noted that the range in composition values was less as the range in physiological maturity among lambs is less. The reason for this comparatively reduced precision in the Beef DEXA system likely reflects the loss of sensitivity of DEXA for differentiating between fat and lean within tissues of greater depth (see MLA project report No P.PIP.0431).

A key improvement since the first report (No P.PIP.0431) was the capacity of the DEXA system to predict composition in the hindquarter, albeit with less precision than in the forequarter, usually describing about 5-10% less of the variation in CT lean%, fat%, and bone%. The previous study was based only upon scans from 8 animals, a factor that may well have limited its power. None-the-less, the ability to predict composition in the hind quarter is a key step forward for this technology.

Lastly, component weight added very little to the precision to the prediction of carcase composition. The only results contrary to this were for the prediction of lean and bone in the hind quarter which demonstrated a small improvement in precision.

6.2 Impact of spray chill and scanning orientation on predicting carcase composition

There was very little difference in carcase composition between spray-chilled and non-spray-chilled carcases. Therefore, it is not surprising that the precision for DEXA to predict composition varied little between sides. The only large differences in precision were for the prediction of CT lean% in the hindquarter with 12-14% better precision in non-spray-chilled carcases, and for the prediction of CT fat% in the hindquarter with 11% better precision in non-spray-chilled carcases.

Similarly, variation in carcase orientation had little impact on the DEXA prediction of carcase composition. No discernible differences could be identified with a 45 degree change in orientation, and even the full 180 degree turn induced only a small difference, and this was only evident in bone. The reason for the small bone-specific effect is not immediately clear, however we can speculate that this may have impacted at the pixel thresholding step in image processing to remove bone-contain pixels. The 180 degree re-orientation may have influenced which pixels were removed, affecting the carcase DEXA value. In practice this scenario is not likely to present a problem as most automated kill chains will ensure a standardised carcase orientation.

These results are important because they imply that variation in spray-chilling practices or small shifts in carcase orientation will have minimal impact on the DEXA measurement. This demonstrates that DEXA will produce highly robust predictions of carcase composition that will not be influenced by variations processing factors making this methodology more transportable under commercial operating conditions.

6.3 Association of DEXA values with the calibration block synthetic phantom

Within the calibration block readings there was relatively little variation in DEXA R-values between scanning times. This meant that there was limited capacity to test for an association between the calibration block and machine variation in carcase R-values. Weak associations were found between calibration block readings and CT lean% and fat% within the forequarter, yet none for the hind quarter. Not surprisingly this lack of variation also meant that correcting the carcase DEXA R-values relative to this block did not improve the prediction of CT composition.

In a positive sense this demonstrates stability in the DEXA readings across the 2 week scanning period. However it should also be noted that this stability may not be seen when installed commercially in abattoirs, with greater fluctuations expected in environmental conditions such as humidity. This was certainly evident within the Bordertown lamb study with calibration block R-values varying by more than double (range = 0.02; see MLA project report No A.MQA. 0017) than was evident within this study (range = 0.008). This highlights the need to re-test the calibration phantom in real-world abattoir conditions where there may well be more substantial drift in DEXA values. Assuming that variation exists, this will then be a relatively simple matter of incorporating a calibration adjustment into future readings.

6.4 Repeatability of DEXA scanning method

In order to assess the repeatability of DEXA values between scans, we undertook two analyses as preliminary indicators of repeatability. However, it should be noted that this study was not specifically designed to test repeatability of DEXA values between scans, with both of these analyses confounded by experimental factors. The first assessed the correlations between the fore and hind sections of the left and right sides of the carcase, in which comparisons were confounded by the presence or absence of spray chilling (left section compared to right section), or by carcase section (fore compared to hind section). The second assessed the correlations between three repeated scans of the same section, but at three different scanning orientations. Despite these obvious experimental confounders, there were strong correlations across all comparisons, particularly for the forequarter comparisons in which correlations were as high as 0.99. Future commercial installations of this DEXA system will be used to examine repeatability in greater detail under industry settings.

6.5 Future work

This report represents the completion of the first phase of calibration of the Beef DEXA system, with an algorithm now available for commercial implementation. However there are a number of tasks required upon initial installation. Firstly device calibration relative to a synthetic calibration block will have to be established in commercial operation. Secondly once additional devices have been installed at other plants around Australia these will require cross validation of the DEXA measurement. And thirdly this system will have to be tested across diverse genotypes to ensure robustness of the composition measurements. This will add to the size and diversity of the calibrating dataset providing industry proof of the reliability of this measurement.

In addition work is on-going to explore more sophisticated image analysis methodologies. This includes regional analyses of pixels within images, as well as further analyses of bone containing pixels to improve the precision of bone composition estimation. While the association of DEXA value with CT bone currently looks very good, estimations of bone muscle and fat content are perfectly correlated given that they stem from a single DEXA value. Establishing a separate DEXA value for bone will uncouple this correlation, an important consideration should producers wish to independently control bone muscle and fat composition genetically.

Lastly we will continue investigating different hardware methodologies with the aim of improving the initial image acquisition. Multi-energy X-ray absorptiometry (MEXA) is one possible avenue of further enhancement, as it may provide better differentiation of R-values across tissue types. The advantage of this if successful, is that it will only require an upgrade of the detectors within the existing imaging system, and cross calibration to tissue phantoms.

7 Conclusion

The Teys DIAB prototype DEXA system demonstrated good potential for predicting CT composition, although this was more precise in the forequarter section of the carcase than the hindquarter. The processing factors that were tested (i.e. spray chilling and carcase orientation) had little impact on these predictions demonstrating the robustness of the system. However more work is required to establish an adjustment for real-world variation in calibration block value. Future analyses will be focused on image processing methodologies to further enhance precision, particularly in the hindquarter.

8 References

Anderson, F, Williams, A, Pannier, L, Pethick, DW, Gardner, GE (2015) Sire carcass breeding values affect body composition in lambs-1. Effects on lean weight and its distribution within the carcass as measured by computed tomography. Meat Science 108, 145-154.

Gundersen, H, Jensen, E (1987) The efficiency of systematic sampling in sterology and its prediction. Journal of Microscopy 147, 229-263.

Gundersen, HJG, Bendtsen, TF, Korbo, L, Marcussen, N, Møller, A (1988) Some new, simple and efficient stereological methods and their use in pathological research and diagnosis pathological research and diagnosis. Acta Pathologica, Microbiologica et Immunologica Scandinavica 96 (1-6), 379-394.

Johnson, ER (1987) Comparison of 12th Rib and Rump Fat Thickness Measurements for Predicting Commercial Beef Yield in Local Market Carcasses. Australian Journal of Experimental Agriculture 27, 613-617.

Johnston, DJ, Reverter, A, Burrow, HM, Oddy, VH, Robinson, DL (2003) Genetic and phenotypic characterisation of animal, carcass, and meat quality traits from temperate and tropically adapted beef breeds. 1. Animal measures. Australian Journal of Agricultural Research 54, 107-118.

Lukaski, HC, Marchello, MJ, Hall, CB, Schafer, DM, Siders, WA (1999) Soft tissue composition of pigs measured with dual x-ray absorptiometry: Comparison with chemical analyses and effects of carcass thicknesses. Nutrition 15, 697-703.

Mercier, J, Pomar, C, Marcoux, M, Goulet, F, Theriault, M, Castonguay, FW (2006) The use of dual-energy X-ray absorptiometry to estimate the dissected composition of lamb carcasses. Meat Science 73, 249-257.

Mitchell, AD, Scholz, AM, Conway, JM (1998) Body composition analysis of small pigs by dual-energy X-ray absorptiometry. Journal of Animal Science 76, 2392-2398.

Mitchell, AD, Solomon, MB, Rumsey, TS (1997) Composition analysis of beef rib sections by dual-energy X-ray absorptiometry. Meat Science 47, 115-124.

Mull, R (1984) Mass estimates by computed tomography: physical density from CT numbers. American Journal of Roentgenology 143, 1101-1104.

Pearce, KL, Ferguson, M, Gardner, G, Smith, N, Greef, J, Pethick, DW (2009) Dual X-ray absorptiometry accurately predicts carcass composition from live sheep and chemical composition of live and dead sheep. Meat Science 81, 285-293.

Peppler, WW, Mazess, RB (1981) Total body bone mineral and lean body mass by dual-photon absorptiometry. I. Theory and measurement procedure. Calcif Tissue Int 33, 353-9.

Pietrobelli, A, Formica, C, Wang, ZM, Heymsfield, SB (1996) Dual-energy X-ray absorptiometry body composition model: Review of physical concepts. American Journal of Physiology-Endocrinology and Metabolism 271, E941-E951.

Suster, D, Leury, BJ, Ostrowska, E, Butler, KL, Kerton, DJ, Wark, JD, Dunshea, FR (2003) Accuracy of dual energy X-ray absorptiometry (DXA), weight and P2 back fat to predict whole body and carcass composition in pigs within and across experiments. Livestock Production Science 84, 231-242.

Watson, R, Polkinghorne, R, Thompson, JM (2008) Development of the Meat Standards Australia (MSA) prediction model for beef palatability. Australian Journal of Experimental Agriculture 48, 1368-1379.